# Graphene-based $TiO_2$ photocatalysts for water decontamination: a brief overview of photocatalytic and antimicrobial performances

**Deepthi John[1,2] and V. Sivanandan Achari[1,*]**

[1]School of Environmental Studies, Cochin University of Science and Technology, Kochi 682 022, India
[2]Department of Chemistry, Deva Matha College, Kuravilangad 686 633, India

**This article highlights the major accomplishments in photocatalytic research and reported-antimicrobial activities of graphene-based titanium dioxide ($TiO_2$) hybrids. Special focus is given to the applications of $TiO_2$–graphene and its major forms ($TiO_2$–graphene oxide and $TiO_2$–reduced graphene oxide) in wastewater treatments. Particularly, for systems envisaged for removing emerging micro-pollutants and microbial pathogens in real-life scenarios. The efficiency of the photocatalysts is found to be influenced by several factors, including the surface, chemical, morphological and interfacial characteristics of the hybrids. The mode of interaction of catalysts with pollutants, the percentage of graphene content and the nature of irradiation sources could alter the expected photocatalytic efficacy. It is concluded that the incorporation of graphene in $TiO_2$ improves its photocatalytic performance by boosting photo-responsiveness and suppressing electron–hole recombination. The oxidative stress by reactive oxygen species and membrane stress due to the material's physico-chemical properties account for the observed antimicrobial activities under controlled conditions of light irradiation.**

**Keywords:** Antimicrobial performance, emerging contaminants, photocatalytic activity, titanium dioxide–graphene nanocomposites, water treatment.

DURING the last decade, a significant amount of work on graphene-based titanium dioxide ($TiO_2$) hybrid nanocomposites has been published. $TiO_2$ is the most commonly employed semiconductor photocatalyst because of its intrinsic qualities such as chemical inertness, photostability, non-toxicity and low cost. When $TiO_2$ is irradiated by UV radiation with energy larger than or equal to its band-gap energy, the valence band electrons are promoted to the conduction band creating hole–electron pairs. These electron–hole pairs are responsible for photocatalytic activity. However, the use of $TiO_2$ in photocatalytic applications is limited for various practical reasons. Compared to the rate of chemical reactions between $TiO_2$ and the adsorbed contaminants, the photogenerated electron–hole pairs recombinate more quickly within $TiO_2$, resulting in low quantum efficiency. Lack of visible light adsorption due to the wide band-gap of $TiO_2$, poor adsorption capacity to hydrophobic pollutants, a strong tendency to aggregate and difficulties in separating $TiO_2$ after the treatment procedure are among the other limitations.

To overcome these limitations and improve the photocatalytic effectiveness of $TiO_2$, numerous methods have been developed, such as metal doping[1], combining with metal oxides[2], quantum dots[3], semiconductors[4] and carbon materials[5]. In particular, there is growing interest in the combination of carbon-based materials such as carbon nanotubes (CNTs)[6], fullerenes[7] and graphene[8] due to their unique physical and chemical properties like easy accessibility, low-cost precursors, high surface area and the resultant increase in active sites on the modified surface, etc. The most important feature is the presence of additional energy levels which will reduce the band-gap and improve the sensitivity to visible light. However, effective carbon doping is difficult to attain as the reaction conditions are to be perfectly followed.

The facile synthesis of graphene from graphite by oxidation has revolutionized its application in developing cutting-edge nanocomposites[9]. Apart from its rich surface properties, graphene suppresses the recombination of the excited charge carriers due to its excellent charge carrier mobility (200,000 $cm^2 V^{-1} s^{-1}$). It also offers a large specific surface area along with excellent thermal and electrical conductivities[10]. It is considered that the photoexcited electrons from $TiO_2$ transfer to graphene, thus suppressing the recombination process. As a result, more reactive oxygen species (ROS) are produced, accelerating pollutant degradation. The $TiO_2$ nanoparticles are anchored to graphene, increasing the effective surface area of the nanocomposites. The surface of the nanocomposites can adsorb more organic pollutants due to the strong $\pi$–$\pi$ interaction between graphene and organic contaminants. In addition, chemical modification of the surface features of graphene allows fine-tuning, which makes it more suitable for composite materials. By combining with graphene, the light absorption range of $TiO_2$ could be extended from the ultraviolet (UV) to the visible region, as graphene reduces the band gap of metal oxide by providing additional energy levels. Thus the integration of $TiO_2$ with graphene promotes photoresponsiveness in the visible region, excellent adsorptivity and charge carrier mobility, all of which could contribute to the photodegradation of contaminants.

*For correspondence. (e-mail: vsachari@cusat.ac.in)

The properties of graphene composites depend on the graphenic material employed in the synthesis. Graphene nanotubes, graphene nanoribbons, graphene oxide (GO) and reduced graphene oxide (RGO) are the major significant varieties reported so far. Among these, GO and its chemically reduced form RGO are the most commonly used. Two-dimensional GO sheets of a few layers thickness are prepared by strong chemical oxidation of graphene, for instance, by modified Hummers method followed by ultrasonic-assisted exfoliation[11]. GO sheets are mostly $sp^2$ hybridized and partially $sp^3$ hybridized carbon atoms with covalently bound oxygen-bearing functional groups like hydroxyl, epoxy and carbonyls. The bonding with these functional groups disturbs the $sp^2$ networks, and GO becomes disordered and loses its conductivity compared with highly ordered graphene. By reducing GO, the $sp^2$ hybrid network can be restored and regain its conductive property. As the reduction leads to substantial changes on the external surfaces, RGO has fewer functional groups than GO.

This article appraises the studies conducted based on the most relevant articles published on graphene/GO/RGO-modified $TiO_2$ composites. Thrust is given on the various applications of composites used explicitly for water decontamination and to identify the current stages of development along with further scope for advanced studies.

## Photocatalytic degradation of pollutants by graphene-based $TiO_2$ composites

Earlier works published in this area are mainly based on the techniques followed for synthesizing graphene-based $TiO_2$ composites. These techniques include the hydrothermal, solvothermal, sol–gel method, sonicated-assisted mechanical mixing, spin coating and electrospinning. The efficacy of the newly developed composites is usually examined for the decomposition of organic contaminants present in water.

### *Photocatalytic degradation of dyes*

Photocatalytic removal of both cationic and anionic dyes, mainly methylene blue (MB), methyl orange (MO) and rhodamine B (RhB), is the most frequently reported method. Though the synthesis and characterization of $TiO_2$–graphene-based composites have been reported earlier[12,13], one of the early prominent works on exploring its photocatalytic activity was by Zhang *et al.*[14]. They prepared a chemically bonded P25–graphene nanocomposite by a single-step hydrothermal method. The produced composite showed photodegradation of MB superior to P25-CNTs. This was attributed to the following reasons: (i) Greater adsorption of MB molecules on the catalyst's surface due to non-covalent $\pi$–$\pi$ conjugation and aromatic regions of graphene. The photogenerated carriers could easily degrade the adsorbed molecules. (ii) Extended photoresponse to the visible region due to narrowing of band gap and good transparency of graphene. The narrowing of band gap was attributed to the strong Ti–O–C chemical bonding. (iii) Suppression of electron–hole recombination. The photoexcited electrons of P25 could be transferred from the conduction band to graphene. Graphene, an efficient acceptor and conductor, might also receive and transport these electrons, forming more reactive species and promoting dye degradation. A large amount of work has been published thereafter, reaffirming the enhanced photodegradation of dyes by $TiO_2$–graphene-based composites prepared using various methods.

According to Jiang *et al.*[15], exposed $TiO_2$ (001) facets play a significant role in the photocatalytic performance of graphene–$TiO_2$ composites for the degradation of MB under UV light. By following a novel hydrofluoric and methanol joint-assisted solvothermal method, they prepared anatase $TiO_2$–graphene with exposed (001) facets, and the enhanced photocatalytic activity of the system was attributed to the effective separation of photoinduced charge carriers and exposure of high energy (001) facets. Similar observations were also made by Wang *et al.*[16]. On the flat anatase (001) facet, all of the Ti atoms were substantially more exposed with a Ti–O–Ti angle of 145° and five coordination. This created several oxygen deficiencies and dioxygen-derived active species were formed due to the preferable adsorption of dioxygen. Since the defective surfaces enable interfacial electron transfer, the parting of photogenerated electron–hole pairs was accelerated by the (001) facets. The loading of GO has to be suitably optimized, failing which excess GO would hinder light absorption by $TiO_2$ and reduce the expected photoactivity. The stability and reusability of the catalyst were also established after running five successive cycles with substantial efficiency. Shah *et al.*[17] synthesized a series of biphasic $TiO_2$–RGO composites with different weight ratios by a green synthetic route starting with $TiCl_4$ and without using any harsh reducing agents. The composite possessed both anatase and rutile phases, and showed enhanced photocatalytic performance towards the degradation of RhB and benzoic acid. The surface areas of the catalysts were increased with the RGO content in the composite, which favoured the adsorption of dye molecules. The $\pi$–$\pi$ interactions among the aromatic regions of RGO and RhB also favoured further adsorption. The photocatalytic activity was maximized at $TiO_2$–2 wt% RGO. The rate constant for the degradation was greater by an order of magnitude than that of P25, following pseudo first-order kinetics.

Byeon and Kim[18] synthesized a continuous gas phase self-assembly of ultrafine $TiO_2$–RGO hybrid flakes with enhanced photocatalytic hydrogen production and dye degradation. Compared to P25–$TiO_2$/L–RGO, the better interfacial contact between the RGO nanoflakes and $TiO_2$ particles facilitated effective electron transfer and improved photocatalytic performance towards the degradation of RhB. Nguyen-Phan *et al.*[19] prepared RGO–$TiO_2$ hybrids with and without chelating agents, viz. triethanolamine and acetylacetone. In the presence of chelating agents, there was

selective growth and uniform distribution of $TiO_2$ nanocrystals on the RGO sheet. The resulting sandwich-like structure exhibited strong coupling and chemical interactions. The increased surface area, reorganized energy levels and enhanced concentration of oxygen vacancies facilitated greater adsorption and efficient degradation of RhB under UV and visible light. The adsorption kinetics was well fitted with the pseudo second-order model, whereas the photocatalytic reaction kinetics obeyed a Langmuir–Hinshelwood pseudo first-order model.

The various forms of $TiO_2$, namely particle, nanotube and nanosheet, also influence the photocatalytic efficiency. Sun *et al.*[20] evaluated the photocatalytic efficiency of P25–graphene, $TiO_2$ nanotube–graphene and $TiO_2$ nanosheet–graphene and reported the superior performance of the latter over the other two. They also probed the RhB photocatalytic degradation mechanism. They carried out a series of radical scavenging studies by adding isopropanol ($^{\bullet}OH$ scavenger) and EDTA–2Na ($h^+$ scavenger), and confirmed that both $^{\bullet}OH$ and $h^+$ had a substantial impact on the degradation mechanism using the three systems in this study. In comparison to the other two systems, $TiO_2$ nanosheet–graphene showed a lower reaction rate in the presence of *p*-benzoquinone ($O_2^{-\bullet}$ radical scavenger), suggesting that $O_2^{-\bullet}$ radical oxidation also contributes significantly to photocatalytic destruction of RhB. This was further confirmed by ESR experiments, where in the DMPO–$^{\bullet}OH$ and DMPO–$O_2^{-\bullet}$ signal intensity steadily improved on exposure to UV radiation. The decreased photo-luminescence (PL) intensity of $TiO_2$ nanosheet–graphene in the steady-state photoluminescence spectra showed better charge transmission across the interface. Time-resolved photoluminescence studies were used for further evaluation of the charge transfer dynamics. Compared to other systems, $TiO_2$ nanosheet–graphene showed the fastest time decay component, almost ten-fold enhancement of electron transfer rate with respect to P25/graphene, proving a more effective interaction and faster electron transfer process across the 2D–2D heterojunction interface. A detailed RhB degradation mechanism was put forward by Byzynski *et al.*[21]. According to the authors, RGO modified the main ROS produced during photocatalytic treatment. Through a series of radical scavenging experiments, they demonstrated that under visible light irradiation, superoxide radical $O_2H^*$ was the main ROS in the photocatalytic decolourization of RhB by both $TiO_2$ and $TiO_2$–RGO heterostructure. However, under UV light, direct photo-oxidation through mono-ionized oxygen vacancies was the primary mechanism for $TiO_2$–RGO, whereas the $O_2H^*$ mechanism still dominated in $TiO_2$. Hydroxyl radical reaction was considered the least essential mechanism in both cases.

Apart from MB, MO and RhB, the degradation of other primary water-polluting dyes has also been reported. These include the sonophotocatalytic degradation of rose bengal by RGO-$TiO_2$ under solar irradiation[22], crystal violet by graphene oxide/Ag/$Ag_2S$–$TiO_2$ nanocomposites under visible light[23], X-3B by graphene–$TiO_2$ continuous fibres under UV irradiation[24], etc.

Many of the reported studies proved that graphene incorporation enhances the photocatalytic performance of $TiO_2$. On compositing with graphene, a reduction in the band gap of $TiO_2$ is observed through the formation of intra-band gap energy levels. According to Li *et al.*[25], an energy-favoured hybridization of O 2*p* and C 2*p* atomic orbitals occurs, enabling the formation of a new valence band. Another explanation is that the *d*-orbital (CB) of $TiO_2$ and $\pi$-orbital of graphene match well in energy levels, have chemical bond interactions and form $d$–$\pi$ electron orbital overlap, which can cause a synergic effect. Therefore, the photoresponsiveness of the composite showed a redshift in the absorption edge and visible light could also be used to generate electron–hole pairs.

The mechanism of photocatalytic degradation of organic pollutants in the presence of graphene-modified $TiO_2$ is well discussed in the literature[21,26–29]. The improved photocatalytic efficiency of the composite is attributed to the strong synergic interactions at the interface between graphene and $TiO_2$. Based on the nature of charge transfer across the interface, three mechanistic pathways are suggested in the literature. They are summarized as follows.

The first mechanism considers the electron transfer from $TiO_2$ to graphene. In the presence of graphene, these photogenerated electrons transfer from the conduction band of $TiO_2$ (*d*-orbital) to the Fermi level of graphene ($\pi$-orbital). Since the CB position of anatase $TiO_2$ is –4.2 eV with a band-gap of about 3.2 eV and the work function of graphene is known to be 4.42 eV, direct transfer of a photoexcited electron from the conduction band of $TiO_2$ to graphene is energetically favourable[13,30]. Good interfacial contact and strong chemical bonds between $TiO_2$ and graphene enable effective electron transfer between them. The excellent conducting and transporting properties of graphene allow these electrons to move freely through the graphene matrix and finally reach the surface to react with water and dissolved oxygen to form ROS such as $O_2^{\bullet-}$, $HO_2^{\bullet}$ and $^{\bullet}OH$ that can effectively oxidize dissolved organic pollutants from aqueous media. The major oxidative species, holes left in the valence band of $TiO_2$, can either react with adsorbed water or surface hydroxyl groups to produce $^{\bullet}OH$ radicals or directly oxidize the organic substrates. The dissociative adsorption of water molecules on the $TiO_2$ surface makes it super hydrophilic, enhancing the efficiency of photocatalytic oxidation and self-cleaning properties. The main photoreaction steps are summarized in eqs (1)–(12) below.

$$TiO_2 \xrightarrow{h\nu} TiO_2\,(e^{-1}{}_{CB}) + TiO_2\,(h^{+}{}_{VB}), \quad (1)$$

$$TiO_2\,(e^{-1}{}_{CB}) + \text{graphene} \rightarrow TiO_2 + \text{graphene}\,(e^{-1}), \quad (2)$$

$$\text{Graphene}\,(e^{-1}) + O_2 \rightarrow \text{Graphene} + O_2^{-\bullet}, \quad (3)$$

$$O_2^{-\bullet} + H^+ \rightarrow HO_2^{\bullet}, \quad (4)$$

$$2HO_2^{\bullet} \rightarrow H_2O_2 + O_2, \quad (5)$$

$$HO_2^{\bullet} + e^{-1} \rightarrow HO_2^{-\bullet}, \quad (6)$$

$$HO_2^{-\bullet} + H^+ \rightarrow H_2O_2, \quad (7)$$

$$H_2O_2 + O_2^{-\bullet} \rightarrow {}^{\bullet}OH + OH^- + O_2, \quad (8)$$

$$H_2O_2 + e^{-1} \rightarrow OH^{\bullet} + OH^-, \quad (9)$$

$$TiO_2\ (h^+_{VB}) + OH^-_{ads} \rightarrow TiO_2 + {}^{\bullet}OH, \quad (10)$$

$$TiO_2\ (h^+_{VB}) + H_2O \rightarrow TiO_2 + H^+ + {}^{\bullet}OH, \quad (11)$$

$${}^{\bullet}OH + RH \rightarrow \text{Degradation products}$$
$$\rightarrow CO_2 + H_2O + \text{other simple inorganic oxides.} \quad (12)$$

Another mechanism by which electrons transfer from graphene to $TiO_2$ is also prevalent. Most theoretical works support electron transfer from graphene to $TiO_2$ (refs 31, 32). The photocatalytic process is initiated by graphene through absorption of visible or UV light. The photoexcited electrons thus formed in the high-energy graphene states are transferred to the $TiO_2$ surface with a nonadiabatic process and then delocalize on the $TiO_2$ structure, which in turn can generate various ROS directly or indirectly[33] (eqs (13)–(15)). Here graphene acts as a macromolecular photosensitizer of $TiO_2$.

$$RGO + h\nu \rightarrow RGO^*, \quad (13)$$

$$RGO^* + TiO_2 \rightarrow RGO + TiO_2\ (e^{-1}_{CB}), \quad (14)$$

$$TiO_2\ (e^{-1}) + O_2 \rightarrow TiO_2 + O_2^{-\bullet}. \quad (15)$$

Both types of charge transfer processes are possible depending on the excitation wavelength used, as it decides the type and energy of the excited levels. Visible light photons can produce charge transfer from graphene to $TiO_2$, whereas the overall charge transfer is in the reverse direction in the case of UV photons[34,35]. In a recent work, Garrafa-Gálvez *et al.*[36] reported that both the mechanisms simultaneously take place during sunlight irradiation of MB, in the presence of RGO–$TiO_2$ where RGO acts as an adsorbent, a charge separator and a photosensitizer at the same time (Figure 1). In any case, both processes produce electron-rich and hole-rich materials enabling photocatalytic oxidation and reduction.

In visible light, a dye-sensitized mechanism has also been suggested for degrading organic dyes. The visible activated dye on the surface of $TiO_2$ can transfer the photoexcited electrons to the $TiO_2$ conduction band or to the electronic diffuse states of RGO. The oxidized dye molecule thus initiates its self-degradation[26].

In general, the photocatalytic performance of $TiO_2$–graphene depends significantly on the interface morphology of the composite, the nature of the organics to be decomposed and the excitation wavelength used. The effectiveness of photocatalysis can be enhanced using composites with substantially improved specific surface area, which can offer more active spots and adsorb more reactive species.

### *Photocatalytic removal of other major pollutants from water*

In addition to dyes, the degradation of other water pollutants like phenolic compounds, pesticides, herbicides, inorganic compounds like heavy metals and refractory materials was also tested with $TiO_2$–graphene-based composites. The enhanced adsorptive as well as photocatalytic removal of phenol by titania/graphene oxide composite compared to the parent materials under UV illumination was reported by Fu *et al.*[37]. The adsorption capacities of phenol on the studied catalysts were in the order $TiO_2$–GO > GO > $TiO_2$ and the absorption kinetics was well fitted by the Langmuir equation, whereas photocatalytic degradation was described by the Langmuir–Hinshelwood pseudo first-order kinetic model. Kim *et al.*[38] studied phenol degradation using an anodized graphene-doped $TiO_2$ nanotube composite under visible light. Compared to pristine $TiO_2$ nanotubes (TNTs), the composite under optimum conditions showed 3.5 times higher degradation rate. The intermediate products identified by TD-GC-MS analysis were propylene glycol, benzene, 1,1′-methylenebis[4-isocyanato-], glycerol, acetone and tetrahydrofuran. The oxidation of phenol into cyclic intermediates like benzene followed by ring-opening reactions to form simpler compounds (e.g. glycerol) and the final mineralization to $CO_2$ and $H_2O$ has been the proposed scheme of degradation. The excellent removal efficiency of alkyl phenols was also reported by Basheer[39].

Contrary to the above results, Minella *et al.*[26] reported that though $TiO_2$–graphene degraded MB at a faster rate (both under UV and visible light), the phenolic degradation occurred only in UV light and was inefficient in visible light. This has been explained based on the earlier reported mechanism that the electrons migrated from the photoexcited state of RGO to titania and holes transferred from titania to RGO. On the surface of RGO, the adsorbed substrates were oxidized. This was possible when the substrate HOMO had higher energy than the empty states of excited RGO that was supposed to be the case for MB and not for phenol. A dye-sensitized mechanism was suggested under visible light, which occurred for MB, not phenol. The increased amount of RGO would decrease the efficiency primarily due to more scattering of light. The RGO reduction degree could influence the energy positions of its LUMO and subsequent electron transfer. The oxygenated functional groups on RGO could be involved in acid–base equilibria that would cause a change in the positions of its Fermi level as a function of pH, thereby altering the positions of the electronic state in comparison with that of $TiO_2$.

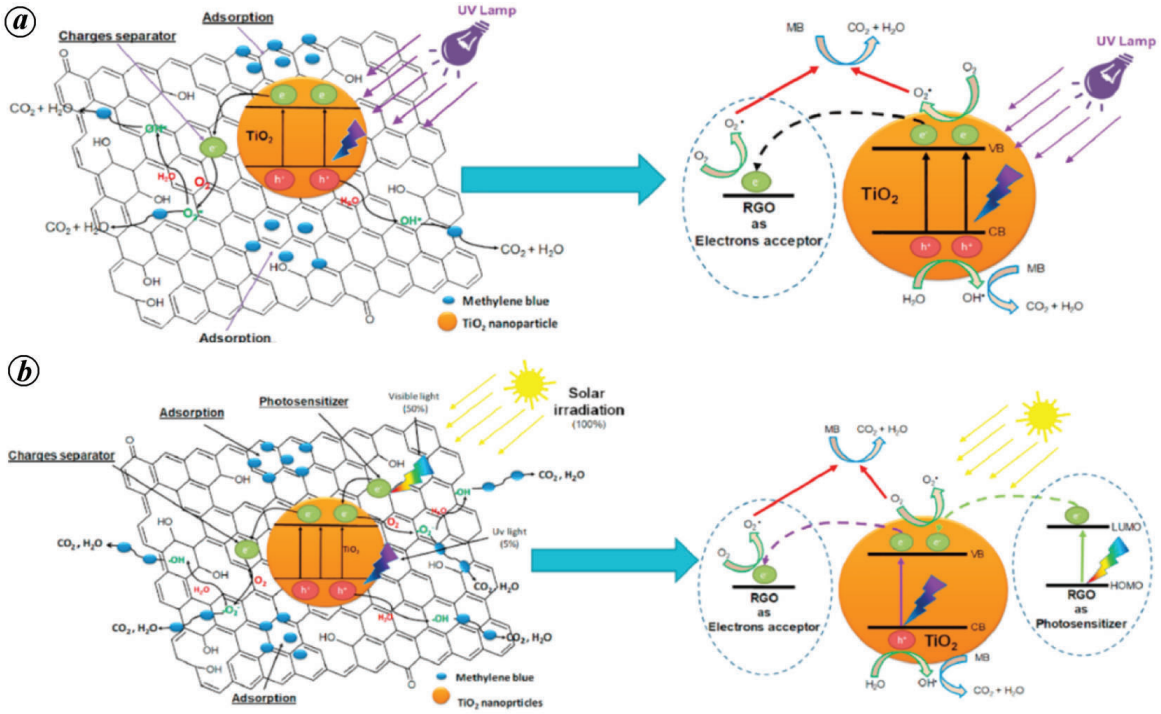


**Figure 1.** Schematic diagram of RGO functions and synergy with $TiO_2$ nanoparticles in the photocatalytic degradation of MB on exposure to (***a***) UV and (***b***) solar radiation[36].

One of the earliest works in this area explored the photoelectrochemical and photocatalytic efficiency of graphene–$TiO_2$ nanocomposites to remove 2,4-dichlorophenoxy acetic acid (2,4-D)[40]. Compared to $TiO_2$, a two-fold increase in photocurrent response and a four-fold enhancement in photocatalytic degradation rate were reported. The better transport properties of graphene, together with the ability of the composite to concentrate the organics near the surface, accounted for the enhanced photocatalytic performance.

The influence of the water matrix (natural and ultrapure water) on the photocatalytic degradation of a mixture of four pesticides, viz. diuron, alachlor, isoproturon and atrazine by $TiO_2$ and GO–$TiO_2$ under UV–Vis and visible radiation was studied by Cruz *et al.*[41]. $TiO_2$ showed decreased degradation in natural water, which was ascribed to the hole-scavenging action of inorganic anions present in natural water. However, GO–$TiO_2$ was less affected by the variation in the water matrix. The lower point of zero charge, $pH_{PZC}$, of the GO–$TiO_2$ compared to $TiO_2$ made the surface negatively charged when natural water of pH ~8 was used, causing less interaction between inorganic anions, thus preventing the scavenging capability of co-occurring materials and hence the inhibitory effect.

The better photocatalytic activity of GO–$TiO_2$ over $TiO_2$ and CNT–$TiO_2$ towards the photocatalytic degradation of a cyanobacterial toxin, microcystin-LA (MC–LA) under both simulated solar and visible light irradiations was reported by Sampaio *et al.*[42]. The GO–$TiO_2$ composite having 4 wt% carbon content showed 88% of MC–LA removal in 2 h.

Naphthenic acid (NA) is one of the major toxic compounds found in oil sands process-affected water, produced during the hot water extraction of bitumen. The extreme stability and complex nature of this compound make its decomposition difficult. Liu *et al.*[43] explored the potential of $TiO_2$ (P25)–graphene for the degradation of NA. A higher removal rate of more than 90% compared to 80% removal rate of P25 was reported by the composite under UV light. The removal rate was more in an acidic medium than in a neutral or alkaline medium. LC-MS analysis showed that macromolecular NAs degraded faster than micromolecular NA.

The suitability of $TiO_2$–RGO as a photocatalyst to treat complex pulp and paper mill effluent has been established by John *et al.*[44]. The integrated process involving coagulation–flocculation and photocatalysis could efficiently remove organics from the effluent with a reduction of over 95% in chemical oxygen demand (COD).

Apart from oxidative removal, reductive removal of metal ions by graphene-based $TiO_2$ composites has also been reported. Reverse osmosis concentrate from wastewater treatment plants contains a high percentage of endocrine-disrupting compounds like heavy metals. Zhang *et al.*[45] studied the photocatalytic removal of $Cd^{2+}$ and $Pb^{2+}$ by $TiO_2$–GO nanocomposites and reported 66.32% and 88.96% removal for $Cd^{2+}$ and $Pb^{2+}$ respectively, under optimum conditions and UV light. Pseudo first-order rate constant showed a 3.75 times increase compared to P25 in both cases. The photocatalyst stability was also proved with excellent removal efficiency even after ten successive cycles. Figure 2 shows a

schematic illustration of the mechanism of heavy-metal reduction[45].

### *Photocatalytic degradation of emerging pollutants*

An emerging environmental problem nowadays is the presence of pharmaceuticals in water bodies. Because of their stability, widespread use and limited human/animal metabolism, these compounds are present at an alarming level in all major water resources. The superior performance of graphene-based $TiO_2$ nanocomposites was explored for the degradation of pharmaceuticals also. Pastrana-Martinez *et al.*[35] studied the degradation of diphenhydramine (DP) with GO–$TiO_2$ composites under near UV/visible light by varying GO loading and calcination temperatures. Complete degradation was achieved for the optimum GO–$TiO_2$ composites calcined at 200°C. Higher calcination temperature (350°C) has negative effects, as this may lead to the breaking of GO–$TiO_2$ bonding. The radical and hole quenching experiments showed that holes were the major reactive species for DP degradation under UV–Vis light, whereas radical-mediated oxidation was observed in visible-light only radiation. The quenching GO–photoluminescence on visible and NIR laser excitation showed that GO acted as an electron acceptor under UV light and as an electron donor and hence a visible light sensitizer of $TiO_2$ under visible light excitation.

Contrary to the above result, Zhang *et al.*[46] reported that RGO–$TiO_2$ composite calcined at 450°C showed improved photocatalytic efficiency. This was attributed to the oxidation of residual organics in the RGO–$TiO_2$ composites as well as to the better crystallized $TiO_2$ with smaller particle sizes.

Bhatia *et al.*[47] studied the degradation of atenolol using GO–$TiO_2$ composite under UV–Vis light and simulated sunlight irradiation, and compared the results with bare $TiO_2$. More improved degradation of atenolol (72%) was achieved at optimum conditions of catalyst concentration (1.50 g/L), pH (6), initial substrate concentration (25 ppm), light intensity and source of light (750 W/cm$^2$ simulated solar irradiation). To ensure complete mineralization, TOC removal was also monitored and complete TOC removal was achieved in 7 h. Compared to the already published results of atenolol degradation, the potential of GO–$TiO_2$ composite for atenolol degradation was thus established without doubt.

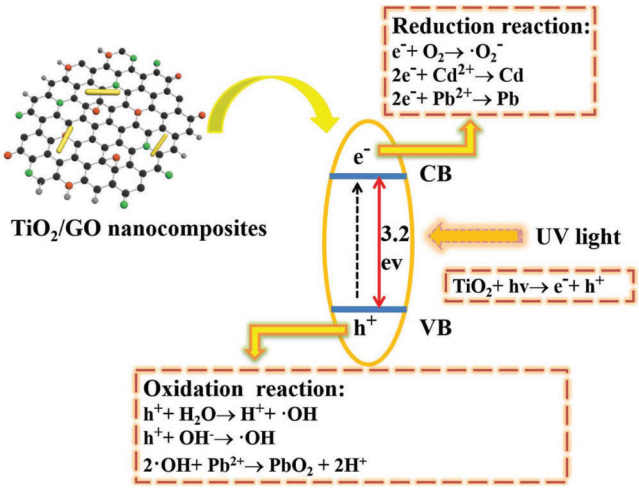


**Figure 2.** Schematic illustration of the transmission of charge and separation in $TiO_2$–GO nanocomposites on exposure to UV radiation and major steps for the reduction of heavy metal ions[45].

In order to have a realistic and more effective application, Karaolia *et al.*[48] conducted a study of the photocatalytic efficiency of RGO–$TiO_2$ in the complex matrix of real urban wastewater under simulated solar irradiation. $TiO_2$–RGO composites were synthesized by two methods, viz. hydrothermal (HD) and photocatalytic treatments (PH), and the efficiency of these varied with the target pollutants. $TiO_2$–RGO–PH was the most efficient for removing antibiotic clarithromycin and erythromycin, while $TiO_2$ outperformed the composites in removing sulphamethoxazole. Complete inactivation of *Escherichia coli* (total and antibiotic-resistant) was achieved after 180 min with all examined photocatalysts and regrowth was absent even after 24 h of post-treatment storage. Among the tested antibiotic-resistant genes, *ampC* (ampicillin resistance gene) was successfully removed and *ecfX* abundance of *Pseudomonas aeroginose* reduced considerably, but *Sul*1 (sulphonamide resistance gene), *erm*B (erythromycin resistance gene) and 23S rRNA for enterococci sequences were persistent. The total genomic DNA content remained stable and resistant to photocatalytic treatment. The water matrices have a significant impact on aqueous phase photocatalysis. Inhibitory elements like dissolved ions and turbidity should be eliminated from the secondary effluent before it is exposed to fine tertiary treatment like photocatalysis[49].

Moreira *et al.*[50] compared different advanced oxidation processes, viz. $H_2O_2$, $TiO_2$–P25, GO–$TiO_2$ and photo-Fenton for removing micropollutants (sulphamethoxazole, carbamazepine and diclofenac), biological contaminants (total *Faecal coliforms* and *enterococci* and their antibiotic-resistant counterparts), 16S rRNA and antibiotic-resistant genes in urban wastewater. The experiments were performed in a solar-driven, pilot-scale CPC photoreactor at Plataforma Solar de Almeria, Spain. P25/$H_2O_2$ was found to be the best method for the removal of both micropollutants and biological contaminants. The better performance of P25 was explained based on the high intensity of UV rays in sunlight. However, heterogeneous photocatalysis using GO–$TiO_2$ also proved useful in removing micropollutants. The addition of $H_2O_2$ increased the photocatalytic efficiency of P25 significantly but reduced the performance of GO–$TiO_2$. This may be due to the degradation of GO–$TiO_2$ by $H_2O_2$ attack to the underlying C–C bonds in the superficial defect sites of GO. All the treatment systems employing $H_2O_2$ could reduce the abundance of total *Faecal coliforms* and enterococci, and their antibiotic-resistant counterparts, and prevent re-emergence even after three days of wastewater storage. However, none of the systems could achieve a permanent reduction in the abundance of the analysed genes.

Lin *et al.*[51] compared the photocatalytic oxidation of pharmaceuticals, viz. ibuprofen, carbamazepine and sulphamethoxazole by $TiO_2$–Fe and $TiO_2$–RGO nanocomposites immobilized on optical fibres. The doping with Fe and RGO decreased the band-gap energy of $TiO_2$ (3.2 eV) to 2.40 and 2.85 eV respectively. $TiO_2$–RGO showed increased photocatalytic ability under UV irradiation, while $TiO_2$–Fe was more suitable for visible light irradiation. The decreased recombination rate of photogenerated carriers accounted for the photocatalytic activity of $TiO_2$–RGO, while the decreased band-gap energy accounted for the efficiency of $TiO_2$–Fe.

Separation and recovery of $TiO_2$-based catalysts from the reactor is a major problem encountered during practical applications. To overcome this, Linley *et al.*[52] reported a modular synthesis of magnetic GO–$TiO_2$ by incorporating $SiO_2$-insulated, nanosized magnetic aggregates. To tackle the current real-world water treatment problems, the degradation of two emerging contaminants, viz. caffeine and carbamazepine, was studied. A rapid removal of caffeine and carbamazepine within 60 min was achieved. Controllable and scalable production methods, easy recovery of the catalyst by a magnetic field, durability and recyclability of the catalyst after multiple trials with little loss of activity and regeneration of activity by simple exposure to UV irradiation were the main features of this work[52].

Photodegradation of famotidine by $TiO_2$–RGO was reported by Gholamvande *et al.*[53]. The better activity of $TiO_2$–RGO in comparison with a mixture of $TiO_2$ and RGO and bare $TiO_2$ was attributed to the better bonding of $TiO_2$ with graphene basal planes. The enhanced settling and filtration properties of the catalyst were the other advantages in industrial applications.

Moranchel *et al.*[54] studied the degradation of clofibric acid, an active metabolite of a pharmaceutical used as a blood lipid regulator, using hydrothermally synthesized $TiO_2$–RGO with different mass ratios. The optical properties were estimated from UV–Vis measurements. With increased RGO content in the studied range of 0.1%–1% w/w, the scattering coefficient in the UV-A range had increased, whereas the absorption coefficient was the lowest. The detrimental effect of excess RGO was attributed to its facilitation of charge carrier recombination. After 6 h of irradiation, clofibric acid was completely degraded. The Monte Carlo method was used to compute the amount of radiation absorbed inside the photocatalytic reactor.

The photocatalytic efficiency of $TiO_2$–RGO catalysts was evaluated for the degradation of risperidone, an antipsychotic drug, under artificial solar and visible light and different aqueous matrices, viz. distilled water, tap water, river water and lake water[55]. Compared to commercial P25, the composite showed higher activity under all aqueous matrices and with both sources of irradiation. The photocatalytic activity of the composite was higher under visible light and showed moderate dependence on the irradiation medium, which decreased in the order: distilled water > tap water > river water > lake water. The transformed products identified by Liquid Chromatography-High Resolution Mass Spectrometry (LC/HRMS) showed the presence of more harmful products. However, faster mineralization guarantees the earlier abatement of toxicity. Lin *et al.*[56] synthesized a series of $TiO_2$–RGO-coated, side-glowing optical fibre (SOF) photoreactors by a polymer-assisted hydrothermal deposition method. The photocatalytic degradation of three pharmaceuticals, including carbamazepine, ibuprofen and sulphamethoxazole was examined under UV–Vis light. The composite showed better photocatalytic activity and the efficiency depended largely on RGO loading, with 2.7% RGO graded as the best. The degradation kinetics fitted well with the Langmuir–Hinshelhood model. The high durability and consistent efficiency made it possible to develop a $TiO_2$–RGO-coated SOFs-mediated continuous flow photoreactor.

### *Antimicrobial activity of $TiO_2$–graphene composites*

One of the early studies on the preparation of $TiO_2$–RGO nanocomposites and the evaluation of their antibacterial property was by Akhavan and Ghaderi[57]. They synthesized GO platelets and deposited them on anatase $TiO_2$ thin films, followed by annealing at 400°C. The UV radiation-assisted photocatalytic reduction caused the conversion of GO to graphene and Ti–C bonding between the components. These high-performance thin films were able to inactivate *E. coli* under solar light. The inactivation efficiency depended strongly on the GO reduction rate and increased by a factor of 7.5 after 4 h reduction compared to the film not subjected to reduction.

Cao *et al.*[58] reported the synthesis of ultrafine $TiO_2$–graphene nanosheets efficient for the inactivation of *E. coli* under indoor natural light irradiation. The visible light-induced photocatalytic activity of the catalyst was attributed to the extended light absorption range, as was evident from the UV absorption spectrum, which showed a redshift in the absorption edge and increased absorption intensity. Again, with graphene being an excellent electron acceptor/transporter, it efficiently separates the photogenerated electrons and holes, which could generate more reactive species capable of causing cell death. However, bare $TiO_2$ as well as the composite showed no antibacterial activity in the absence of light. Similar results were also reported by Kandiah *et al.*[59], where the $TiO_2$–graphene nanocomposites showed no bactericidal and bacteriostatic activities in *E. coli* and *Staphylococcus aureus*. This was explained as due to the ineffective interaction between the bacterial cell wall and material surface, as this determined the intrinsic antimicrobial property of a material to a greater extent. Apart from the role of ROS, the major effect of surface characteristics in the photocatalytic inactivation of *E. coli* was also discussed by Wanag *et al.*[60]. They claimed that the change in surface charge of $TiO_2$ from zeta potential negative to positive when incorporated with graphene would enhance its interaction with the negatively charged *E. coli* surface. Figure 3 shows SEM images of *E. coli* at different stages of inactivation.

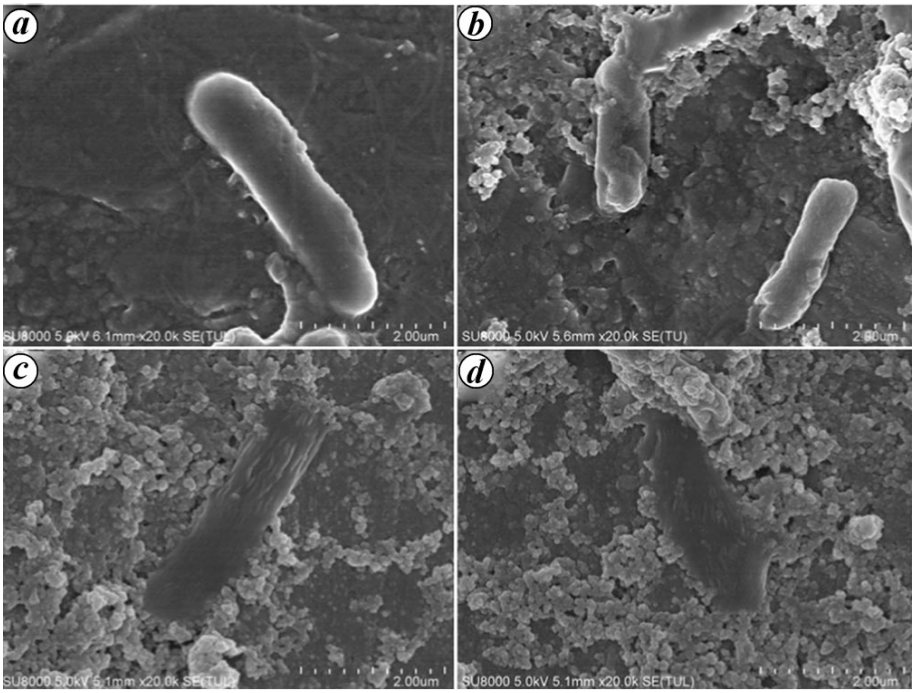


**Figure 3.** SEM images of (***a***) *Escherichia coli* bacterium cell, (***b***) bacterial cell coated with $TiO_2$–RGO–1.5 prior to ASL irradiation, (***c***, ***d***) bacterial cell damaged after exposure of 75 min (ref. 60).

Functional nanomaterials based on biopolymers are of great interest to the scientific community due to their improved bio-functions. Liu *et al.*[61] synthesized GO–$TiO_2$ in a matrix of bacterial cellulose (BC). The properties of BC like high tensile strength, Young's modulus, crystallinity, excellent water-holding capacity and biocompatibility could be used to develop new disinfectants with environmental and medical applications. The GO–$TiO_2$ nanocomposites retained their photocatalytic and antibacterial properties even after being incorporated into the BC matrix. The antibacterial activity of this material was assessed for the inactivation of *S. aureus* cells under near UV radiation and maximum activity with the antibacterial rate of 91.3% was achieved. The effect of calcination temperature on photocatalytic efficiency was also evaluated. A calcination temperature of 450°C was found best for photocatalytic efficiency. The highly conductive graphene and the porous structure of $TiO_2$ formed at higher temperatures increased the photoelectric conversion efficiency. The decreased efficiency at lower (400°C) and higher (>450°C) calcination temperatures was ascribed to the presence of a higher portion of amorphous $TiO_2$ and the anatase to rutile transformation in $TiO_2$ respectively. The decreased surface area due to the growth of $TiO_2$ crystallites at higher calcination temperatures also negatively affected the photocatalytic performance. The intracellular accumulation of ROS was monitored by measuring the fluorescence intensity of the fluorescent probe DCFH-DA (2,7-dichlorodi-hydrofluorescein diacetate). The enhanced antibacterial activity was associated with increased intracellular ROS production. The free-radical scavenging experiments conducted in the presence of the antioxidant glutathione considerably increased the *S. aureus* cells survival rate. Thus, the oxidative stress caused by ROS was confirmed as the underlying mechanism for the decrease in cell viability and apoptotic death.

The photocatalytic and antibacterial activity of $TiO_2$–graphene composites can be further improved by incorporating metal ions in the hybrid system. Multifunctional GO–$TiO_2$–Ag reported by Liu *et al.*[62] exhibited excellent photocatalytic activation in degrading AO7 and phenol under solar irradiation. The composite also showed intrinsic antibacterial activity towards *E. coli* due to Ag nanoparticles. The enhanced photocatalytic bacterial inactivation of the ternary system compared to GO–$TiO_2$ and GO–Ag was attributed to Ag nanoparticles, which could significantly suppress the recombination of photoinduced electrons and holes. The antibacterial activity of Ag–$TiO_2$–graphene under visible light towards diarrhoea-causing pathogen *Campylobacter jejuni* was reported by Noreen *et al.*[63]. Decreased motility, cellular leakage of protein and DNA, hydrophobicity and auto-aggregation of *C. jejuni* were proved experimentally. Bacterial cell damage was confirmed by Atomic Force Microscopy (AFM) images (Figure 4). The composite inhibited biofilm formation. As no significant cytotoxicity was observed against the human neuroblastoma cell line, safe use of the nanoparticle in antibiofilm coating material was established. Similar results were also published by Yang *et al.*[64] for bifunctional $TiO_2/Ag_3PO_4$/graphene composites. The excellent bactericidal effect was attributed to the intrinsic bacterial inactivation of $Ag_3PO_4$ and photoinduced antibacterial

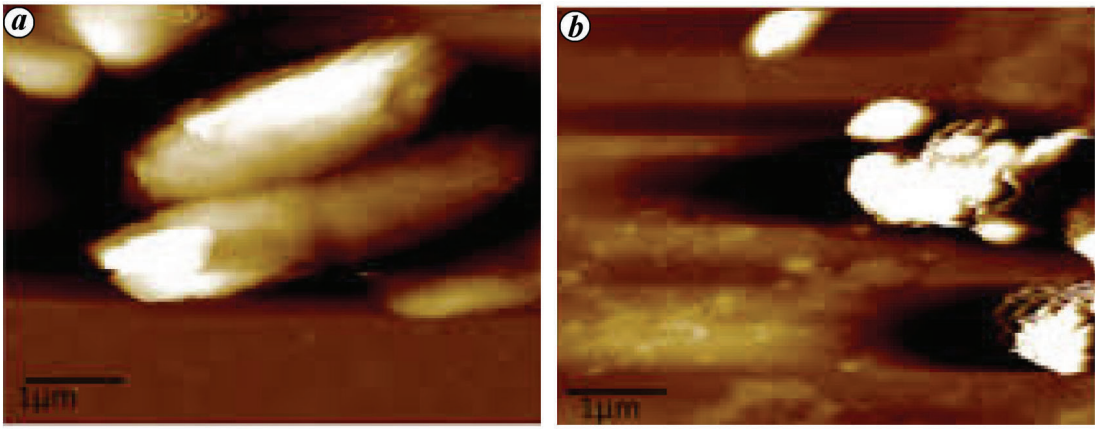


**Figure 4.** Impact of $TiO_2$/GR/Ag nanocomposite on *Campylobacter jejuni* cellular morphology. ***a***, Control (untreated) sample showing cells with smooth and intact boundaries. ***b***, Treated sample exhibiting cells with imperfect boundaries and leakage[63].

activity due to ROS generated in the visible light-irradiated system.

Au–$TiO_2$ nanocomposites on monolayer graphene were synthesized by He *et al.*[65] and tested for their photocatalytic performance for the degradation of methyl orange and bacterial inactivation of a Gram-negative bacterium (*E. coli* K12), a Gram-positive bacterium (*R. palustris*) and a fungus (Candida) under solar irradiation. The superior performance of the composite was probed by biomolecule oxidation measurements which suggested that both oxidative burst of the membrane and destruction of the antioxidant systems were the main reasons. A theoretical support for the relationship between photocatalytic activity and antibacterial properties based on perturbation theory, radiation theory and Schottky barrier theory was also provided by the authros[65]. The rates of charge transfer and electron–hole recombination were studied. They linked transportation and separation of electron–hole pairs to the range of optical absorption and barrier height respectively.

Chang *et al.*[66] reported the synthesis of magnetic GO–$TiO_2$ (MGO–$TiO_2$) for the first time by incorporating iron in the composite. Among the three different compositions, MGO–$TiO_2$ having 6.02% Fe exhibited 100% antibacterial activity against *E. coli* after 30 min solar irradiation with 180 mg/L of the composite. They also found that the addition of inorganic ions such as $HCO_3^-$, $HPO_4^{2-}$, $SO_4^{2-}$, $Cl^-$, $NO_3^-$, $K^+$ and $Na^+$ reduced the antibacterial inactivation, $HCO_3^-$ and $HPO_4^{2-}$ having the most pronounced influence[66]. It was explained that $HCO_3^-$ and $HPO_4^{2-}$ could react with $^{\bullet}OH$ radicals and reduce the number of ROS. The saturation magnetization of the system was 33.87 emu/g and only 16.30 emu/g was sufficient for magnetic separation, the black catalyst particles could be easily separated by applying a magnetic field. It was also reported that incorporating oxidants like persulphate in the $TiO_2$–RGO photocatalytic system could improve its bactericidal activity[67]. This has been attributed to the increased production of ROS generated in the presence of persulphate and the subsequent high levels of oxidative attacks on bacteria.

A few works have been reported recently where the antibacterial properties of $TiO_2$–graphene-based materials were utilized for real-life applications. To extend the use to food packaging applications, different polyvinyl alcohol (PVA)-based polymer nanocomposite films were made by Dhanasekar *et al.*[68], incorporating unmodified $TiO_2$ and $Cu_2O$–$TiO_2$/RGO. Compared to PVA–$TiO_2$, PVA–$Cu_2O$–$TiO_2$/RGO was more effective for the inactivation of *E. coli*, *Pseudomonas aeruginosa*, *S. aureus* and *S. oralis*, with *S. aureus* showing the highest inactivation. Stan *et al.*[69] developed RGO–$TiO_2$ nanocomposite-coated cotton fabrics with antibacterial and self-cleaning properties, which are harmless to human skin cells. Several carbon and nanometal oxide–carbon composites are used for decontamination purposes; their prospective response to photocatalytic activities is yet to be determined[70–72].

Cruz-Ortiz *et al.*[73] conducted a detailed mechanistic study of the ROS-mediated inactivation of *E. coli* under UV–Vis and visible-only radiation using $TiO_2$–P25 and $TiO_2$–RGO as photocatalysts. Various ROS probes and scavengers were used to study the mechanism of disinfection of *E. coli*. The major ROS detected were $H_2O_2$, $^{\bullet}OH$ radicals and singlet oxygen ($^1O_2$) under UV–Vis irradiation, whereas singlet oxygen alone was detected under visible-only illumination. The improved performance of $TiO_2$–RGO over $TiO_2$–P25, GO and RGO was attributed to the increased production of these ROS in the presence of $TiO_2$–RGO. The non-identification of superoxide radicals, which are usually formed by the oxidation of molecular oxygen, was due to the rapid oxidation to singlet oxygen by the mid-gap states created by Ti–C bonds. An interesting result was obtained during the detection of $H_2O_2$ using NaCl solution instead of distilled water as the aqueous medium. A decrease in the concentration of $H_2O_2$ formed was noted in the NaCl solution compared to distilled water. The chloride ions got oxidized by mid-gap states to chlorine which could successively react

with $H_2O_2$ generating singlet oxygen. Figure 5 shows the possible mechanisms for the formation of ROS[73].

To summarize, the antibacterial activities of $TiO_2$–graphene-based hybrid materials depend on nanoscale distribution, composition, structure, surface characteristics and properties of the individual constituents. The adhesion/deposition of microorganisms on the surface of the material will promote effective interfacial interactions. Once good contact is established, the material triggers membrane stress leading to cytoplasm leakage and cell death. Another important factor is the oxidative stress induced by ROS, which disrupts cellular processes and destroys cellular structure. In short, oxidative stress due to ROS and membrane stress due to the specific physico-chemical properties of the material are the two major aspects of the antibacterial activity of $TiO_2$–RGO materials.

## Conclusion

Major outcomes of the significant studies in the area of graphene-based $TiO_2$ photocatalysts for water treatment have been reviewed here. On compositing with graphene, band gap energy of $TiO_2$ was reduced due to the interaction between the 3*d*-orbital of $TiO_2$ and $\pi$-orbital of graphene. This enhances the visible light response of the catalyst. The photogenerated electrons in $TiO_2$ could move freely to graphene, and these as well as the holes formed in $TiO_2$, in reaction with water/dissolved oxygen, gave rise to ROS, which are necessary for initiating photodegradation. Moreover, graphene can act as a visible light-sensitizer promoting photocatalytic degradation. The efficiency of the photocatalytic process depends on a number of factors, such as the morphology of the composite, the type of bonds existing at the interface, the method of interaction between the composite and pollutant, the nature and amount of graphenic material (graphene, GO, RGO), etc. Functionalized graphenes are more reactive than pristine graphene in $TiO_2$ composites. The composites with exposed (001) active facet could accelerate the photogenerated separation of electrons and holes. The increased surface area as well as the altered surface charge of the composite on incorporating graphene will facilitate the selective adsorption of pollutants. The photocatalytic process is found to proceed through ROS-mediated mechanism, of which $^{\bullet}OH$-initiated degradation is considered the most dominant. Though most of the earlier works tested the photocatalytic activity of the composites under laboratory conditions by selecting dyes as model pollutants, recent works explore the potential of these composites in removing emerging micropollutants present in real wastewater systems. The excellent photoinduced antimicrobial activity of these composites finds applications in the inactivation of pathogens in wastewater as well as in the development of functionalized antimicrobial materials. Studies using natural sunlight as the light source have also been reported recently. However, further studies are inevitable in designing and developing more solar-based techniques for large-scale industrial applications, as they reduce adverse environmental impacts and are cost-effective. These are the ultimate aim of any photocatalytic process.

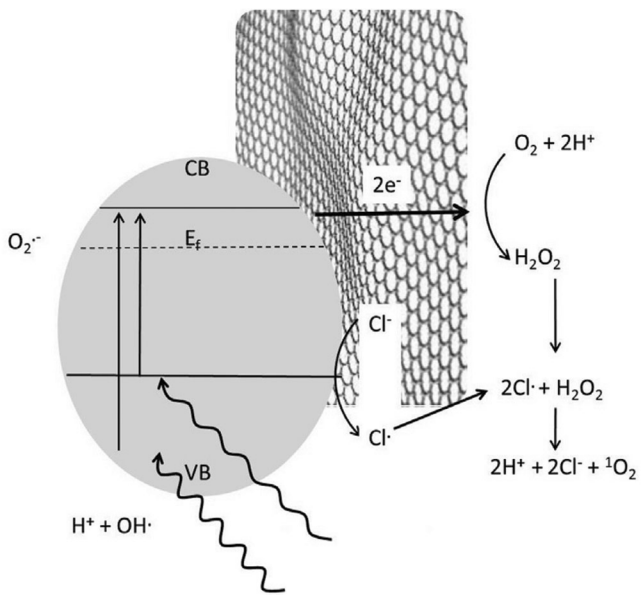


**Figure 5.** Mechanism of photocatalytic ROS production on $TiO_2$–RGO on exposure to UV and visible radiation in the presence of chloride[73].


1. Bhatia, V. and Dhir, A., Transition metal doped $TiO_2$ mediated photocatalytic degradation of anti-inflammatory drug under solar irradiations. *J. Environ. Chem. Eng.*, 2016, **4**, 1267–1273.
2. Ola, O. and Maroto-Valer, M. M., Transition metal oxide based $TiO_2$ nanoparticles for visible light induced $CO_2$ photoreduction. *Appl. Catal. A*, 2015, **502**, 114–121.
3. Martins, N. C. T., Ângelo, J., Girão, A. V., Trindade, T., Andrade, L. and Mendes, A., N-doped carbon quantum dots/$TiO_2$ composite with improved photocatalytic activity. *Appl. Catal. B*, 2016, **193**, 67–74.
4. Chung, J., Kim, S.-R. and Kim, J.-O., Fabrication and characterization of CdS doped $TiO_2$ nanotube composite and its photocatalytic activity for the degradation of methyl orange. *Water Sci. Technol.*, 2015, **72**, 1341–1347.
5. Wu, G., Nishikawa, T., Ohtani, B. and Chen, A., Synthesis and Characterization of carbon-doped $TiO_2$ nanostructures with enhanced visible light response. *Chem. Mater.*, 2007, **19**, 4530–4537.
6. Shahrezaei, F., Pakravan, P., Azandaryani, A. H., Pirsaheb, M. and Mansouri, A. M., Preparation of multi-walled carbon nanotube-doped $TiO_2$ composite and its application in petroleum refinery wastewater treatment. *Desalin. Water Treat.*, 2016, **57**, 14443–14452.
7. Da Meng, Z. *et al.*, Fullerene modification CdSe/$TiO_2$ and modification of photocatalytic activity under visible light. *Nanoscale Res. Lett.*, 2013, **8**, 1–10.
8. Bhanvase, B. A., Shende, T. P. and Sonawane, S. H., A review on graphene–$TiO_2$ and doped graphene–$TiO_2$ nanocomposite photocatalyst for water and wastewater treatment. *Environ. Technol. Rev.*, 2017, **6**, 1–14.
9. Lawal, A. T., Graphene-based nano composites and their applications – a review. *Biosens. Bioelectron.*, 2019, **141**, 111384.
10. Zhu, Y. *et al.*, Graphene and graphene oxide: synthesis, properties, and applications. *Adv. Mater.*, 2010, **22**, 3906–3924.
11. Deshmukh, S. P., Kale, D. P., Kar, S., Shirsath, S. R., Bhanvase, B. A., Saharan, V. K. and Sonawane, S. H., Ultrasound assisted preparation of RGO/$TiO_2$ nanocomposites for effective photocatalytic degradation

of methylene blue under sunlight. *Nanostruct. Nano-objects*, 2020, **21**, 100407.
12. Lambert, T. N. *et al.*, Synthesis and characterization of titania–graphene nanocomposites. *J. Phys. Chem. C*, 2009, **113**, 19812–19823.
13. Williams, G., Seger, B. and Kamat, P. V., $TiO_2$–graphene nanocomposites. UV-assisted photocatalytic reduction of graphene oxide. *ACS Nano*, 2008, **2**, 1487–1491.
14. Zhang, H., Lv, X., Li, Y., Wang, Y. and Li, J., P25–graphene composite as a high performance photocatalyst. *ACS Nano*, 2010, **4**, 380–386.
15. Jiang, B. *et al.*, Enhanced photocatalytic activity and electron transfer mechanisms of graphene/$TiO_2$ with exposed {001} facets. *J. Phys. Chem. C*, 2011, **115**, 23718–23725.
16. Wang, W. S., Wang, D. H., Qu, W. G., Lu, L. Q. and Xu, W., Large ultrathin anatase $TiO_2$ nanosheets with exposed {001} facets on graphene for enhanced visible light photocatalytic activity. *J. Phys. Chem. C*, 2012, **116**, 19893–19901.
17. Shah, M. S. A. S., Park, A. R., Zhang, K., Park, J. H. and Yoo, P. J., Green synthesis of biphasic $TiO_2$-reduced graphene oxide nanocomposites with highly enhanced photocatalytic activity. *ACS Appl. Mater. Interfaces*, 2012, **4**, 3893–3901.
18. Byeon, J. H. and Kim, Y., Gas-phase self-assembly of highly ordered titania@graphene nanoflakes for enhancement in photocatalytic activity. *ACSAppl. Mater. Interf.*, 2013, **5**, 3959–3966.
19. Nguyen-Phan, T. D. *et al.*, Uniform distribution of $TiO_2$ nanocrystals on reduced graphene oxide sheets by the chelating ligands. *J. Colloid Interf. Sci*., 2012, **367**, 139–147.
20. Sun, J., Zhang, Guo, L. and Zhao, L., Two-dimensional interface engineering of a titania–graphene nanosheet composite for improved photocatalytic activity. *ACS Appl. Mater. Interf.*, 2013, **5**, 13035–13041.
21. Byzynski, G. D., Volanti, P., Ribeiro, C., Mastelaro, V. R. and Longo, E., Direct photo-oxidation and superoxide radical as major responsible for dye photodegradation mechanism promoted by – $TiO_2$–rGO heterostructure. *J. Mater. Sci. Mater. Electron*., 2018, **29**, 17022–17037.
22. Rosy, A. and Kalpana, G., Influence of RGO/$TiO_2$ nanocomposite on photo-degrading Rhodamine B and rose bengal dye pollutants. *Bull. Mater. Sci*., 2018, **41**, 2–9.
23. Shuang, S., Lv Ruitao, Cui, X., Xie, Z., Zheng, J. and Zhang, Z., Efficient photocatalysis with graphene oxide/Ag/$Ag_2S$–$TiO_2$ nanocomposites under visible light irradiation. *RSC Adv*., 2018, **8**, 5784–5791.
24. Zhang, Q. *et al.*, Advanced fabrication of chemically bonded graphene/$TiO_2$ continuous fibers with enhanced broadband photocatalytic properties and involved mechanisms exploration. *Sci. Rep.*, 2016, **6**; https://doi.org/10.1038/srep38066/.
25. Li, K. *et al.*, Design of graphene and silica co-doped titania composites with ordered mesostructure and their simulated sunlight photocatalytic performance towards atrazine degradation. *Colloids Surf. A*, 2013, **422**, 90–99.
26. Minella, M., Sordello, F. and Minero, C., Photocatalytic process in $TiO_2$/graphene hybrid materials. Evidence of charge separation by electron transfer from reduced graphene oxide to $TiO_2$. *Catal. Today*, 2017, **281**, 29–37.
27. Nosaka, Y. and Nosaka, A. Y., Generation and detection of reactive oxygen species in photocatalysis. *Chem. Rev*., 2017, **117**, 11302–11336.
28. Wang, X., Zhang, J., Zhang, X. and Zhu, Y., Characterization, uniformity and photo-catalytic properties of graphene/$TiO_2$ nanocomposites via Raman mapping. *Opt. Express*, 2017, **25**, 21496–21508.
29. Kusiak-Nejman, E. *et al.*, Graphene oxide–$TiO_2$ and reduced graphene oxide–$TiO_2$ nanocomposites: insight in charge-carrier lifetime measurements. *Catal. Today*, 2017, **287**, 189–195.
30. Lightcap, I. V., Kosel, T. H. and Kamat, P. V., Anchoring semiconductor and metal nanoparticles on a two-dimensional catalyst mat. Storing and shuttling electrons with reduced graphene oxide. *Nano Lett*., 2010, **10**, 577–583.
31. Ferrighi, L., Fazio, G. and Di Valentin, C., Charge carriers separation at the graphene/(101) anatase $TiO_2$ interface. *Adv. Mater. Interf.*, 2016, **3**, 1–7.
32. Yu, S. *et al.*, Complex roles of solution chemistry on graphene oxide coagulation onto titanium dioxide: batch experiments, spectroscopy analysis and theoretical calculation. *Sci. Rep*., 2017, **7**, 1–10.
33. Long, R., English, N. J. and Prezhdo, O. V., Photo-induced charge separation across the graphene–$TiO_2$ interface is faster than energy losses: a time-domain ab initio analysis. *J. Am. Chem. Soc*., 2012, **134**, 14238–14248.
34. Gillespie, P. N. O. and Martsinovich, N., Electronic structure and charge transfer in the $TiO_2$ rutile (110)/graphene composite using hybrid DFT calculations. *J. Phys. Chem. C*, 2017, **121**, 4158–4171.
35. Pastrana-Martínez, L. M. *et al.*, Advanced nanostructured photocatalysts based on reduced graphene oxide–$TiO_2$ composites for degradation of diphenhydramine pharmaceutical and methyl orange dye. *Appl. Catal. B*, 2012, **123–124**, 241–256.
36. Garrafa-Gálvez, H. E. *et al.*, Graphene role in improved solar photocatalytic performance of $TiO_2$–RGO nanocomposite. *Chem. Phys*., 2018, **521**, 35–43.
37. Fu, C. C., Juang, R. S., Huq, M. M. and TeHsieh, C., Enhanced adsorption and photodegradation of phenol in aqueous suspensions of titania/graphene oxide composite catalysts. *J. Taiwan Inst. Chem. Eng*., 2016, **67**, 338–345.
38. Kim, S. R., Ali, I. and Kim, J. O., Phenol degradation using an anodized graphene-doped $TiO_2$ nanotube composite under visible light. *Appl. Surf. Sci*., 2019, **477**, 71–78.
39. Basheer, C., Application of titanium dioxide–graphene composite material for photocatalytic degradation of alkylphenols. *J. Chem*., 2013; https://doi.org/10.1155/2013/456586.
40. Ng, Y. H., Lightcap, I. V., Goodwin, K., Matsumura, M. and Kamat, P. V., To what extent do graphene scaffolds improve the photovoltaic and photocatalytic response of $TiO_2$ nanostructured films? *J. Phys. Chem. Lett*., 2010, **1**, 2222–2227.
41. Cruz, M. *et al.*, Bare $TiO_2$ and graphene oxide $TiO_2$ photocatalysts on the degradation of selected pesticides and influence of the water matrix. *Appl. Surf. Sci*., 2017, **416**, 1013–1021.
42. Sampaio, M. J. *et al.*, Carbon-based $TiO_2$ materials for the degradation of microcystin-LA. *Appl. Catal. B*, 2015, **170–171**, 74–82.
43. Liu, J., Wang, L., Tang, J. and Ma, J., Photocatalytic degradation of commercially sourced naphthenic acids by $TiO_2$–graphene composite nanomaterial. *Chemosphere*, 2016, **149**, 328–335.
44. John, D., Yesodharan, S. and Achari, V. S., Integration of coagulation–flocculation and heterogeneous photocatalysis for the treatment of pulp and paper mill effluent. *Environ. Technol*., 2022, **43**, 443–459; https://doi.org/10.1080/09593330.2020.1791972.
45. Zhang, H. *et al.*, Synthesis and characterization of $TiO_2$/graphene oxide nanocomposites for photoreduction of heavy metal ions in reverse osmosis concentrate. *RSC Adv*., 2018, **8**, 34241–34251.
46. Zhang, Y., Hou, X., Sun, T. and Zhao, X., Calcination of reduced graphene oxide decorated $TiO_2$ composites for recovery and reuse in photocatalytic applications. *Ceram. Int*., 2016, **43**, 1150–1159.
47. Bhatia, V., Malekshoar, G., Dhir, A. and Ray, A. K., Enhanced photocatalytic degradation of atenolol using graphene $TiO_2$ composite. *J. Photochem. Photobiol. A*, 2017, **332**, 182–187.
48. Karaolia, P. *et al.*, Removal of antibiotics, antibiotic-resistant bacteria and their associated genes by graphene-based $TiO_2$ composite photocatalysts under solar radiation in urban wastewaters. *Appl. Catal. B Environ*., 2018, **224**, 810–824.
49. John, D., Rajalakshmi, A. S., Lopez, R. M. and Achari, V. S., $TiO_2$-reduced graphene oxide nanocomposites for the trace removal of diclofenac. *SN Appl. Sci*., 2020, **2**, 840.
50. Moreira, N. F. F. *et al.*, Solar treatment ($H_2O_2$, $TiO_2$–P25 and GO–$TiO_2$ photocatalysis, photo-Fenton) of organic micropollutants, human pathogen indicators, antibiotic resistant bacteria and related genes in urban wastewater. *Water Res*., 2018, **135**, 195–206.

51. Lin, L., Wang, H., Jiang, W., Mkaouar, A. R. and Xu, P., Comparison study on photocatalytic oxidation of pharmaceuticals by $TiO_2$–Fe and $TiO_2$–reduced graphene oxide nanocomposites immobilized on optical fibers. *J. Hazard. Mater*., 2017, **333**, 162–168.
52. Linley, S., Liu, Y., Ptacek, C. J., Blowes, D. W. and Gu, F. X., Recyclable graphene oxide-supported titanium dioxide photocatalysts with tunable properties. *ACS Appl. Mater. Interf*., 2014, **6**, 4658–4668.
53. Gholamvande, Z., Morrissey, A., Nolan, K. and Tobin, J., Graphene/$TiO_2$ nano-composite for photocatalytic removal of pharmaceuticals from water. In Proceedings of IWAWCE-2012 Conference; http://keynote.conference-services.net/resources/444/2653/pdf/iwawce2012_0244.pd
54. Moranchel, A., Manassero, A., Satuf, L., Alfano, O. M., Casas, A. and Bahamonde, A., Influence of $TIO_2$–rGO optical properties on the photoctalytic activity and efficiency to photodegrade an emerging pollutant. *Appl. Catal. B*, 2019, **246**, 1–11.
55. Calza, P. *et al.*, Photocatalytic transformation of the antipsychotic drug risperidone in aqueous media on reduced graphene oxide–$TiO_2$ composites. *Appl. Catal. B*, 2016, **183**, 96–106.
56. Lin, L., Wang, H. and Xu, P., Immobilized $TiO_2$-reduced graphene oxide nanocomposites on optical fibers as high performance photocatalysts for degradation of pharmaceuticals. *Chem. Eng. J*., 2017, **310**, 389–398.
57. Akhavan, O. and Ghaderi, E., Photocatalytic reduction of graphene oxide nanosheets on $TiO_2$ thin film for photoinactivation of bacteria in solar light irradiation. *J. Phys. Chem. C*, 2009, **113**, 20214–20220.
58. Cao, B., Cao, S., Dong, P., Gao, J. and Wang, J., High antibacterial activity of ultrafine $TiO_2$/graphene sheets nanocomposites under visible light irradiation. *Mater. Lett*., 2013, **93**, 349–352.
59. Kandiah, K., Muthusamy, P., Mohan, S. and Venkatachalam, R., $TiO_2$–graphene nanocomposites for enhanced osteocalcin induction. *Mater. Sci. Eng. C*, 2014, **38**, 252–262.
60. Wanag, A. *et al.*, Antibacterial properties of $TiO_2$ modified with reduced graphene oxide. *Ecotoxicol. Environ*., 2018, **147**, 788–793.
61. Liu, L.,Yang, X., Ye, L., Liu, M., Jia, S., Hou, Y. and Chu, L., Preparation and characterization of a photocatalytic antibacterial material: graphene oxide/$TiO_2$/bacterial cellulose nanocomposite. *Carbohydr. Polym*., 2017, **174**, 1078–1086.
62. Liu, L., Bai, H., Liu, J. and Sun, D. D., Multifunctional graphene oxide–$TiO_2$–Ag nanocomposites for high performance water disinfection and decontamination under solar irradiation. *J. Hazard. Mater*., 2013, **261**, 214–223.
63. Noreen, Z., Khalid, N. R., Abbasi, R., Javed, S., Ahmad, I. and Bokhari, H., Visible light sensitive Ag/$TiO_2$/graphene composite as a potential coating material for control of *Campylobacter jejuni*. *Mater. Sci. Eng. C*, 2019, **98**, 125–133.
64. Yang, X., Qin, J., Jiang, Y., Rong, Li., Yang, Li. and Tang, H., Bi-functional $TiO_2$/$Ag_3PO_4$/graphene composites with superior visible light photocatalytic performance and synergistic inactivation of bacteria. *RSC Adv*., 2014, **4**, 18627–18636.
65. He, W. *et al.*, Photocatalytic and antibacterial properties of Au–$TiO_2$ nanocomposite on monolayer graphene: from experiment to theory. *J. Appl. Phys*., 2013, **114**, 204701.
66. Chang, Y., Ou, X., Zeng, G., Gong, J. and Deng, C., Synthesis of magnetic graphene oxide–$TiO_2$ and their antibacterial properties under solar irradiation. *Appl. Surf. Sci*., 2015, **343**, 1–10.
67. John, D., Jose, J., Bhat, S. G. and Achari, V. S., Integration of heterogeneous photocatalysis and persulfate based oxidation using $TiO_2$-reduced graphene oxide for water decontamination and disinfection. *Heliyon*, 2021, **7**; https://doi.org/10.1016/j.heliyon.2021.e07451.
68. Dhanasekar, M. *et al.*, Ambient light antimicrobial activity of reduced graphene oxide supported metal doped $TiO_2$ nanoparticles and their PVA-based polymer nanocomposite films. *Mater. Res. Bull*., 2018, **97**, 238–243.
69. Stan, M. S. *et al.*, Reduced graphene oxide/$TiO_2$ nanocomposites coating of cotton fabrics with antibacterial and self-cleaning properties. *J. Ind. Text.*, 2019, **49**, 277–293.
70. Achari, V. S., Lopez, R. M., Rajalekshmi, A. S., Jayasree, S., Ravindran, B. and Sekkar, V., Scavanging nitrophenol from aquatic effluents with triethyl amine catalyzed ambient pressure dried carbon aerogel. *J. Environ. Chem. Eng*., 2020, **8**, 103760; https://doi.org/10.1016/j.jece.2020.103670.
71. Achari, V. S., Lopez, R. M., Rajalakshmi, A. S., Jayasree, S., Shibin, O. M., John, D. and Sekkar, V., Microporous carbon with highly dispersed nano-lanthanum oxide ($La_2O_3$) for enhanced adsorption of methylene blue. *Sep. Purif. Technol*., 2021, **279**, 119626; https://doi.org/10.1016/j.seppur.2021.119626.
72. Achari V. S., Lopez, R. M., Jayasree, S. and Rajalakshmi, A. S., Lanthanum ion impregnated granular activated carbon for the removal of phenol from aqueous solution: equilibrium and kinetic study. *Int. J. Chem. Kinet.*, 2019, **51**, 215–231; https://doi.org/10.1002/kin.21245.
73. Cruz-Ortiz, B. R. *et al.*, Mechanism of photocatalytic disinfection using titania–graphene composites under UV and visible irradiation. *Chem. Eng. J*., 2017, **316**, 179–186.


Received 10 May 2020; accepted 21 June 2022

doi: 10.18520/cs/v123/i9/1089-1100